Sixty year ^{10}Be record from Greenland and Antarctica

A ALDAHAN[1,2], G POSSNERT[2], S J JOHNSEN[3], H B CLAUSEN[3], E ISAKSSON[4], W KARLÉN[5] and M HANSSON[6]

[1]*Institute of Earth Sciences, Uppsala University, S-752 36 Uppsala, Sweden*
[2]*Tandem Laboratory, Uppsala University, S-751 21 Uppsala, Sweden*
[3]*Geophysical Institute, University of Copenhagen, Copenhagen D-2200 Denmark and Science Institute, University of Iceland, IS-107 Reykjavik, Iceland*
[4]*Norwegian Polar Institute, Box 5072, N-0301 Oslo, Norway*
[5]*Department of Physical Geography, Stockholm University, S-106 91, Stockholm, Sweden*
[6]*Department of Meteorology, Stockholm University, S-106 91 Stockholm, Sweden*

We report in this study the distribution of ^{10}Be in the top 40 m of the Renland ice core (East Greenland) and in a 30 m long core from DML (Dronning Maud Land, Antarctica) for the period 1931–1988. The two sites show differences in ^{10}Be content, the Antarctica site showing smaller variance and a lower average ^{10}Be annual flux. Similarly, the average accumulation rate (cm water equivalent year^{-1}) is higher in the Renland relative to DML. The variability in accumulation (precipitation) rates seems to explain part of the difference in ^{10}Be flux between the two polar sites. Cyclic fluctuations of ^{10}Be flux correlate with the 11-year sunspot number and cosmic ray intensity than with the aa index (perturbation of the geomagnetic activity by the solar wind). Our data corroborate ^{10}Be cyclic fluctuation pattern from the Dye 3 ice core and confirm a promising potential for correlation of global and local events.

1. Introduction

High resolution climatic records often show inter-annual signals which could be a result of a number of causes. One example is the variation in the world-wide air and sea surface temperature and precipitation that appears to correlate with the 11-year solar activity cycle (Currie 1987; Royer 1993; Stuiver *et al* 1995). Currie (1994) and Seleshi *et al* (1994) presented further evidence for a correlation between heavy rainfall/flood events and the solar cycle. In spite of this correlation, the extrapolation to future meteorological forecasts is uncertain, mostly due to the relatively short and consequently poorly understood solar activity archives. Polar ice sheets provide one of the best natural records for documentation of climate change and they have, together with tree rings, been used to retrieve data on past solar activity (Lal 1987; Beer *et al* 1990; Stuiver and Braziunas 1993; Stuiver *et al* 1995). Among other parameters (e.g. oxygen isotopes), the distribution of ^{14}C and/or ^{10}Be are the main sources of information about past solar activity. However, unlike the case with ^{14}C where several long records are available for annual calibration and correlation, only one long record is available for ^{10}Be (from Dye 3 in Greenland; Beer *et al* 1990). Recently two other short records from Antarctica (Dronning Maud Land; Aldahan *et al* 1995 and Taylor Dome; Steig *et al* 1996) and one from Greenland (Renland; Aldahan *et al* 1995) were presented. Although the Dye 3 is an excellent record, questions were raised whether all parts of the record reflect the sun activity or are affected by climatic and/or ice dynamics (Stuiver and Braziunas 1993). It thus seemed important to capture the ^{10}Be-solar cycles in other cores from Greenland and to test the feasibility on cores from Antarctica. This study aims at such an approach for spatial and temporal correlations of global and local climate events, snow accumulation rates and ice dynamics. Furthermore, the extraction of annual-based ^{10}Be

Keywords. Antarctica; Be-10; Greenland; ice; solar activity; climate.

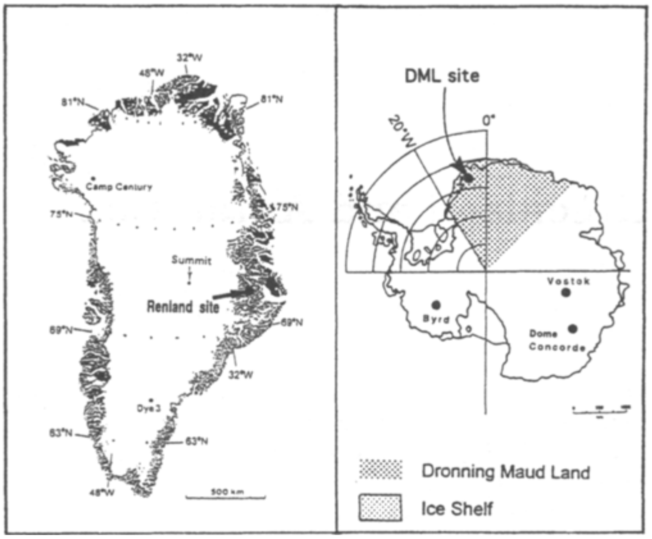

Figure 1. Location map of the sites for cores used in this study.

record from Antarctica provides potential for testing the mode of transfer of short term signals between the two hemispheres and a possible extension over time periods longer (e.g. through the Maunder Minima) than the one used in this work.

2. Material and methods

Two cores were used in this study (figure 1), namely the top 40 m of the Renland ice core, East Greenland, 71°18′N-26°43′W (Johnsen *et al* 1992) and a 30 m long core taken about 200 km from the coast line in Dronning Maud Land, DML (73°36′S-12°26′W), Antarctica (for details of site description and coring see Isaksson *et al* 1996). The cores consist of firn without pronounced melt layers. However, thin ice layers, typically a few millimeters thick, occur occasionally and are most likely formed during days with intense solar radiation. There are no indications of severe melting and percolation of meltwaters at these sites.

The cores were sliced on an annual basis using physical boundaries, oxygen isotopes and tritium chronology. The oxygen isotope measurements were made at the Geophysical Institute, Copenhagen University (Denmark) for the Renland core and at the Stable Isotope Laboratory, University of Maine (USA) for the Antarctic ice. Tritium analysis was made at the Institute of Earth Sciences, Uppsala University. ^{10}Be was extracted from the filtered (through 0.45 µ filter) samples (250–1300 ml water) by a cation column separation after addition of 150 µg ^{9}Be-carrier and the result is expressed in atoms/gram

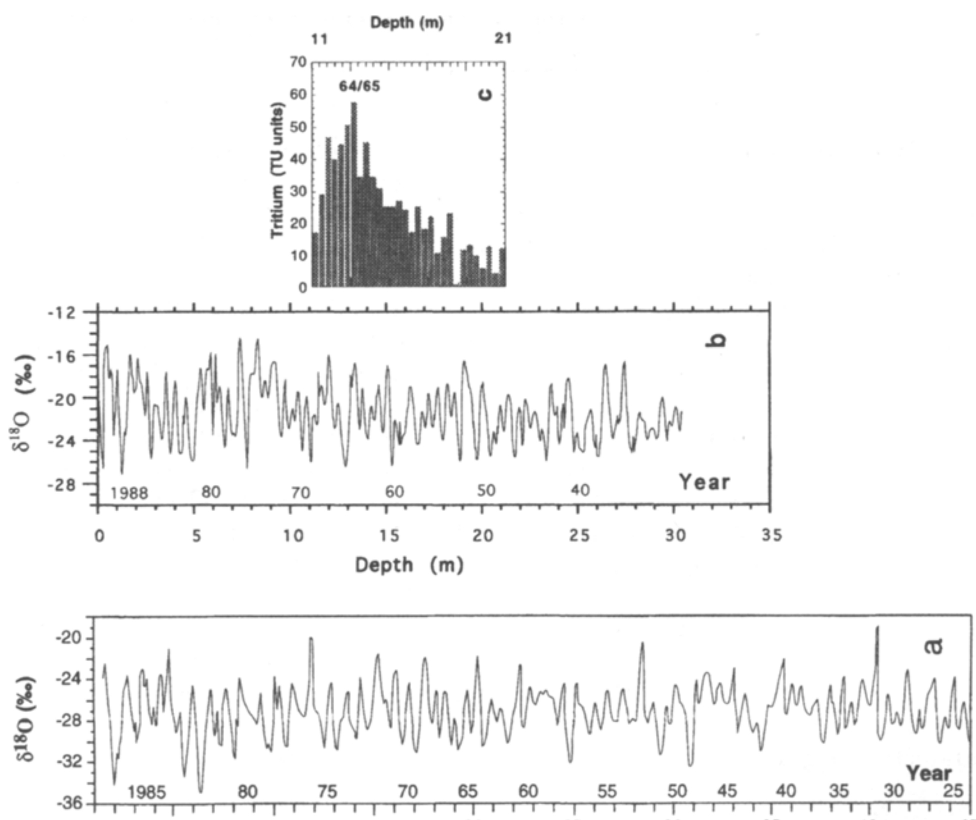

Figure 2. The $\delta^{18}O$ (relative to SMOW) profiles of Renland (**a**) and the Dronning Maud Land (**b**) cores. (**c**). The tritium profile of a part of the Dronning Maud Land core, the analytical error as 1 standard deviation is ±6 TU.

water. The measurement was made with the 6 MV EN-tandem accelerator (at Uppsala University) and absolute $^{10}Be/^{9}Be$ values were established relative to the NIST reference standard SRM 4325. Details of the preparation and measurement of ^{10}Be are given in Aldahan and Possnert (1993a and b). The total error in ^{10}Be data (including machine stability, analysis statistics) is < 5% (one standard deviation) but may reach 15% upon correction for boron.

3. Results and interpretations

A rather clear seasonal variation is apparent in the $\delta^{18}O$ of the Renland core for the period 1931–1987 (figure 2a) with an average mean value of about −27.4‰ and maximum and minimum of −19.0‰ and −34.9‰ respectively. Similarly, obvious seasonal variation, average −21‰, maximum −14.5‰ and minimum −27.2‰, is observed by the $\delta^{18}O$ of the DML core (figure 2b). The tritium data (figure 2c), showed elevated activity at a depth of 12.5–14 m that indicates the bomb peak of 1963/1964 and this was used to partly adjust the $\delta^{18}O$ time scale by a shift of two years. Based on this chronology, estimates of annual accumulation rates for the DML site vary from about 16 to 79 cm water equivalent year^{-1} (cm w. eq. y^{-1}) with an average of about 32 whereas the range and average for the Renland site are 22–72 and 45 cm w. eq. y^{-1}, respectively.

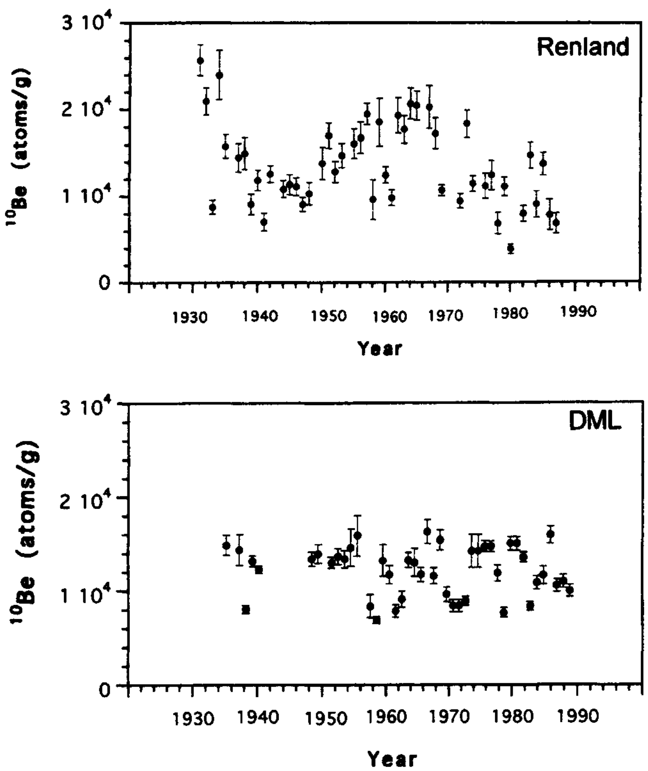

Figure 3. The ^{10}Be concentration in Renland and Dronning Maud Land (DML) cores.

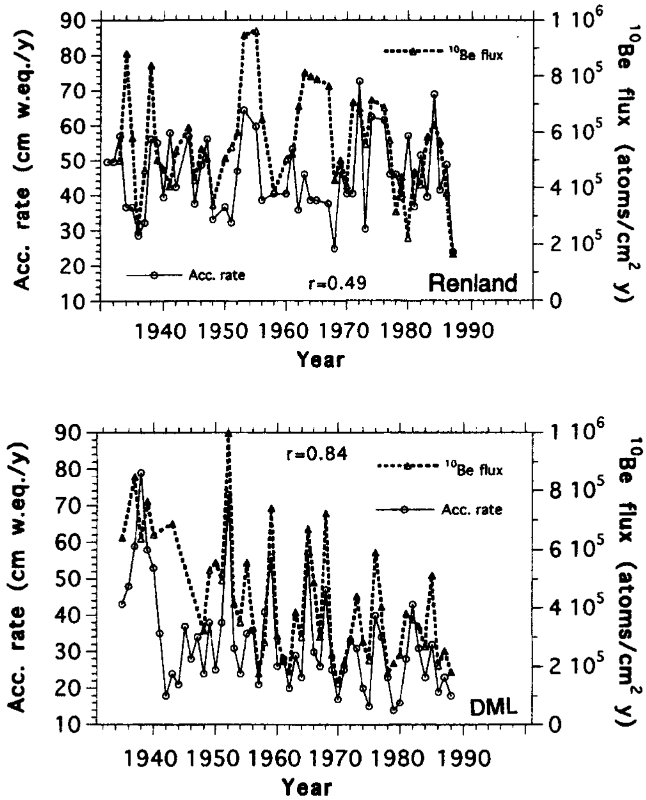

Figure 4. The correlation between ^{10}Be flux and accumulation rate in the Renland and DML. The value of correlation coefficient for a linear regression fit to the data is shown as r.

^{10}Be results indicate a larger scatter of concentrations in the Renland core relative to the DML core (figure 3) for the analysed time period; the ranges are ≈ 0.38–2.6×10^4 atoms g^{-1} and ≈ 0.7–2.9×10^4 atoms g^{-1}, respectively (Appendix 1). However, most data points are confined between ≈ 0.7 and 2×10^4 atoms g^{-1} and the average value of $\approx 1.3\times10^4$ atoms g^{-1} is estimated for both sites. It is to mention that this average value does not change significantly (1.4×10^4 and 1.2×10^4 atoms g^{-1} for the Renland and DML respectively) upon excluding the points with large errors (see Appendix 1). In both data sets, there is also apparent fluctuations. Comparison of our absolute ^{10}Be concentrations with earlier published results (though the latter include effects of different standards used in different laboratories), indicates a higher upper level (mostly $\approx 2\times10^4$ atoms g^{-1}) in the cores studied here than the reported for Dye 3, $\approx 1.1\times10^4$ atoms g^{-1}, (Beer *et al* 1990) of the same time period. On the other hand, the ^{10}Be concentration range of the Taylor Dome (Steig *et al* 1996) is comparable to the range in our cores (figure 3), though less scatter is found in the DML core.

To compensate for variability produced by snow accumulation rate, we have calculated the ^{10}Be flux (figure 4) as atoms cm^{-2} year^{-1}; flux $=^{10}Be$ concentration (atoms g^{-1})× accumulation rate (cm w. eq y^{-1})

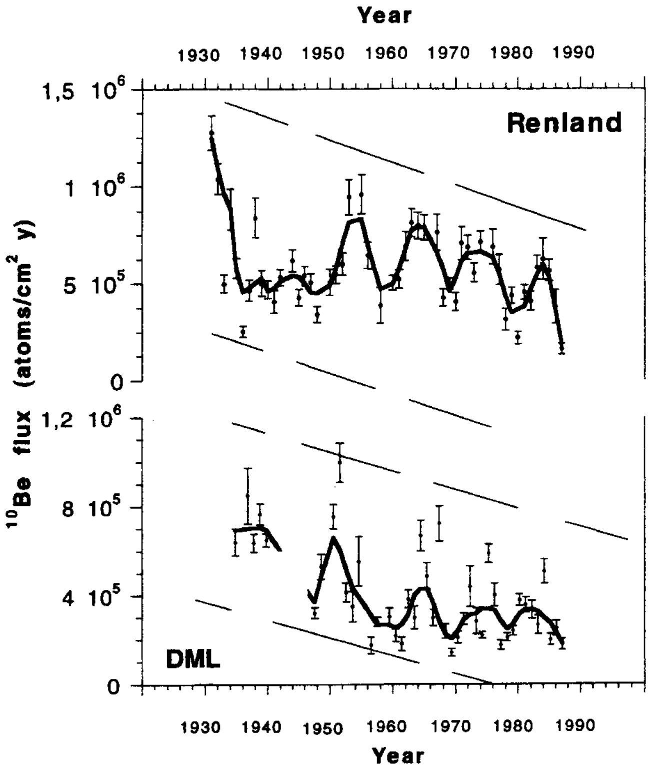

Figure 5. The ^{10}Be flux rate (calculated relative to accumulation rate water equivalent) in Renland and Dronning Maud Land (DML) cores. The line fits are 14% weighted average smoothing of the data series. Five points (1957 and 1959 of the Renland that show flux above 1.3×10^6 atoms cm^{-2} $year^{-1}$ and 1943, 1950 and 1959 of the DML that have odd position) were excluded in order to give comparable range to the smoothing function. The smoothing method used is called locally weighted regression scatter plot smoothing. The method uses a tricube function for curve fitting that gives smaller weighting to the smoothed points at the edges of a smoothed strip. Mathematical treatment and details of the method are given in Chambers (1983). The dashed lines show the general trend of the ^{10}Be flux (for details see text).

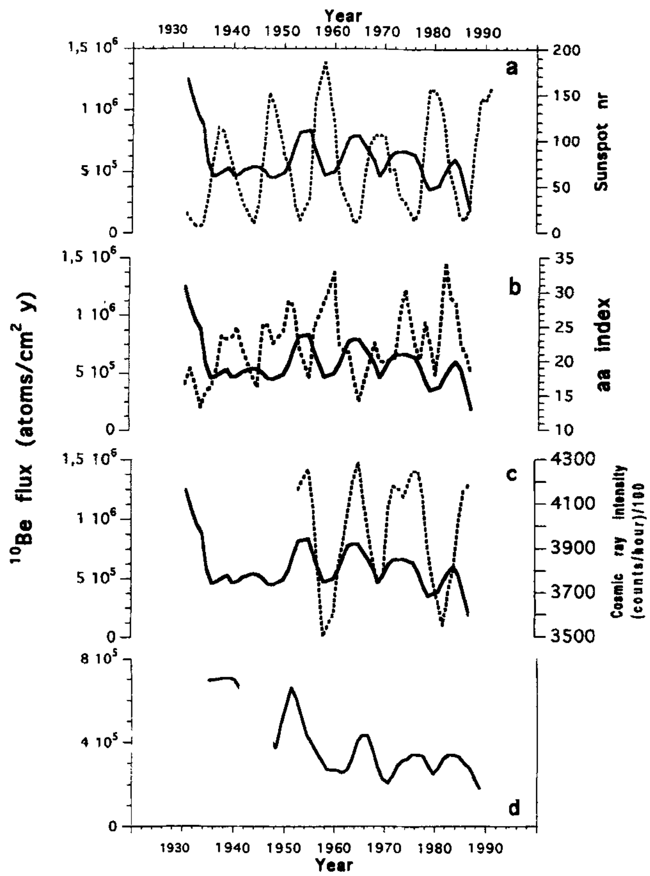

Figure 6. Correlation between sunspot number (**a**: dotted line) aa index (**b**: dotted line; data of Beer *et al* 1990 and references therein) and (**c**: dotted line) cosmic ray intensity (neutron monitor, Climax, Colorado as provided by the solar-geophysical data reports of the National Oceanic and Atmospheric Administration 1994) and ^{10}Be flux of the Renland (a, b and c, solid line) and of the Dronning Maud Land (**d**).

$\times 1$ (water density g cm^{-3}). Both cores show similar flux range (≈ 1.4–10×10^5 atoms cm^{-2} $year^{-1}$) with the exception of three samples (1931, 1957 and 1959; see Appendix 1) from the Renland core that show flux values higher than 12×10^5 atoms cm^{-2} $year^{-1}$. Excluding these three samples, the average flux is $\approx 5.5 \pm 0.6 \times 10^5$ atoms cm^{-2} $year^{-1}$ for the Renland and $\approx 4.2 \pm 0.3 \times 10^5$ atoms cm^{-2} $year^{-1}$ for the DML. Correlation between ^{10}Be flux and accumulation rate (figure 4) indicates stronger positive value (linear regression correlation $r = 0.89$) for the DML relative to the Renland ($r = 0.51$). The flux data indicate a generally decreasing trend (dashed lines in figure 5) towards the present.

Although the range of scatter in the data points became smaller and fluctuations are better revealed by using ^{10}Be flux rather than concentration (figure 5), there are still, however, some points that appear as outliers (1936 and 1938 in the Renland, and 1952, 1965, 1968 and 1985 in the DML). The sources for these outliers are difficult to evaluate, but a potential candidate might be extreme local meteorological variation such as storms with redistribution of snow (figure 5). We have smoothed out the data by using a weighted-average-function and the fit to both sets seems comparable (figure 5). The smoothing reveals pronounced cycles that span about 11 years, but because of the larger year-to-year scatter in the distribution of the DML flux data, the amplitude of the cycles was slightly suppressed. The Renland and DML records are not adjusted for the hemispheric seasonal shift.

The annual ^{10}Be flux together with the variability of the annual solar activity (sunspot number), aa index (perturbation of the geomagnetic activity induced by solar wind), and cosmic ray intensity (neutron monitor) are plotted in figure 6(a-d). In these figures, there is about 1–2 year lag between the ^{10}Be time scale and the solar geophysical data because of the about 1–2 year residence time of ^{10}Be in the atmosphere, differences in hemispheric seasons and a delay in signal (decrease/increase in production/flux) transfer between the two polar regions. Thus, for example, a ^{10}Be data point referred to as 1980 in the Renland core will be equivalent to 1981 in the DLM core, but the ^{10}Be signal would reflect production of 1978/1979 or the earlier year. Consequently, the ^{10}Be data show partly delayed and partly overlapping signals when compared with the solar geophysical data. Regardless of this complexity, the flux of ^{10}Be indicates an obvious negative correlation with the sunspot number (figure 6a and d) and a positive correlation with the cosmic ray intensity (figure 6c and d). The correlation of ^{10}Be flux with the aa index shows, however, a complex pattern (figure 6b and d). In the top part of the records (1989–1970), the aa index is positively correlated with the ^{10}Be flux and in the rest is negatively correlated. The reason(s) for this variability is discussed below.

4. Discussion and conclusions

As has been pointed out by several studies, the variability of cosmogenic ^{10}Be in ice cores relates to variability in atmospheric production and/or climatic conditions (Beer *et al* 1990; Lal 1987; Lal and Jull 1992; Stuiver and Brazinunas 1993; Stuiver *et al* 1995). Based on ^{10}Be concentration, the data of this study show similarity in the ranges (≈ 0.7–2×10^4 atoms g^{-1}) and averages ($\approx 1.3 \times 10^4$ atoms g^{-1}) between the Greenland and Antarctica sites. The flux data (normalized to precipitation as water equivalent), however, indicate that the Renland site has about 30% higher flux ($5.5 \pm 0.6 \times 10^5$ atoms cm^{-2} $year^{-1}$) compared with the DML site ($4.2 \pm 0.3 \times 10^5$ atoms cm^{-2} $year^{-1}$). Similarly, the estimates of annual ^{10}Be fall out made by Lal (1987) also show a higher average value ($\approx 5.2 \times 10^5$ atoms cm^{-2} $year^{-1}$) in Greenland relative to ($\approx 4 \times 10^5$ atoms cm^{-2} $year^{-1}$) Antarctica. Our data of precipitation (or accumulation rate as water equivalent) indicate about 40% higher average accumulation rate in Renland (45 cm w. eq.y^{-1}) relative to that in DML (32 cm. w.eq. y^{-1}). However, the positive corrrelation between ^{10}Be flux and accumulation rate (figure 4) is more significant in the DML and indicates that, at least, part of the variability in the flux relates to variabilty in accumulation rate. Although the cause of this correlation is not obvious, a tentative explanation is frequent occurrence of storms and cyclones that provide a higher supply of ^{10}Be at these relatively near coast sites.

The range of ^{10}Be flux (≈ 0.2–1×10^6 atoms cm^{-2} $year^{-1}$) of the studied polar sites is lower than the average global production rate of $1.2 \pm 0.7 \times 10^6$ atoms cm^{-2} $year^{-1}$ at middle latitudes (Monaghan *et al* 1986). Although higher production rates are calculated for the polar relative to middle latitudes, the pattern of stratospheric/tropospheric air mass circulation enhance deposition (fall out) at the middle latitudes (Lal and Peters 1967). Lal (1987) calculated a factor of three attenuation in the amplitude of middle latitude's flux at latitude 70° which increases with higher latitudes. This seems to explain the difference between the estimates of global average production and the flux at polar regions. The $\approx 5.5 \pm 0.6 \times 10^5$ atoms cm^{-2} $year^{-1}$ flux of the Renland (lat. 71°) is comparable with the Lal's (1987) fall out estimates of 5.7 and 5.9×10^5 atoms cm^{-2} $year^{-1}$ at the Crete (lat. 71°) and Milcent (lat. 70°) respectively, but higher than the about 4.1×10^5 atoms cm^{-2} $year^{-1}$ for the Camp Century (lat. 77°). This latitude attenuation effect is also indicated by the comparable flux data of our core and Lal's fall out estimates for Antarctica sites (3.9–4.4×10^5 atoms cm^{-2} $year^{-1}$; DML, lat. 73°, Dome C, lat. 74° and Vostok, lat. 78°). Steig *et al* (1996) suggested that direct stratospheric input explains the variability of ^{10}Be flux at the Taylor Dome and they assume that only 35% of the total ^{10}Be flux is supplied from low-to-mid latitude stratosphere.

As the records used in this study extend over relatively short time periods, we do not try to get into

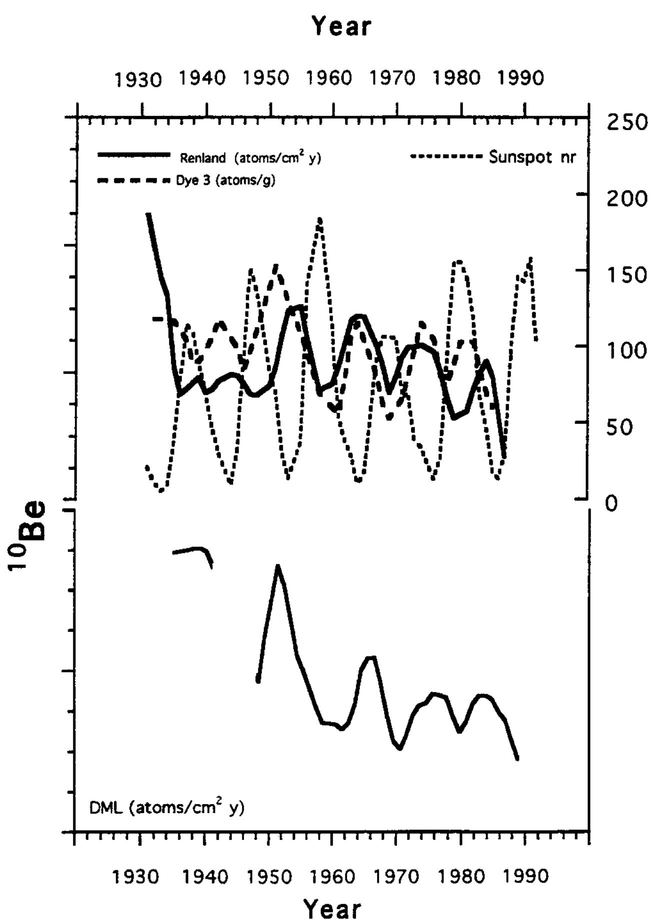

Figure 7. Correlation between ^{10}Be of Renland, Dronning Maud Land (DML) and Dye 3 cores and sunspot number.

refined statistical correlations in order to evaluate the temporal effect of regional (dust, moisture source, snow movements) and global (latitudinal) contributions. However, the rather good match between the pattern of ^{10}Be flux and the 11-year solar activity (sunspot number) and cosmic ray intensity (neutron monitor) (figure 6b and c) suggests that most of the modulation effect on ^{10}Be production is controlled by these two factors. Although, these two factors are anticorrelated and the intensity of cosmic rays incident on the earth is strongly modulated by the solar wind, part of the modulation is also related to the geomagnetic field strength (Lal 1992). The calculation of Lal (1992) indicates that increase in the relative intensity of the dipole field has more pronounced effect on the ^{10}Be production than relative increase in solar activity. This seems to be one possible explanation for the complex and rather poor match between the ^{10}Be flux and the aa index. However, there is a clear decreasing trend in the flux of ^{10}Be toward 1988 in our records (figure 5, dashed lines) and the records of Dye 3 and Taylor Dome. This may relate to the effect of an envelope of a larger (e.g. 61 or 88 year) solar forcing cycle (Stuiver *et al* 1995).

Also as shown by figure 6(a and d), inspite of good cycle correlation, there is no clear correspondence between the solar activity range and ^{10}Be flux range, an observation also made by Beer *et al* (1990) for the ^{10}Be concentration of Dye 3. Maximum and minimum values in ^{10}Be flux do not follow those of the solar activity record. The general range in ^{10}Be flux of our data is a factor of ≈ 6, whereas the range of the general modulation intensity (expressed as O (MV) by Lal 1992) is a factor of ≈ 3 for the analysed time period. This difference in the ratios may be related to change in ^{10}Be production due to the effect of the relative change in the dipole field intensity, cosmic ray flux, and/or climatic (accumulation rate) influence. These effects, together with some disturbance due to the shift (lag/overlap) in the signal because of ^{10}Be residence time, make the possibility of directly isolating the magnitude of each factor on ^{10}Be production complicated. For example, flux recorded during the period 1950–1954 is relatively higher than the later periods in both our records as well as in the concentration record of Dye 3 (figure 7), though the solar activity was not the lowest. However, Steig *et al* (1996) suggested that stratospheric ^{10}Be could contribute significantly ($\approx 65\%$) to their record from the Taylor Dome. Their conclusion was based on the relatively large difference in the amplitude of ^{10}Be concentration between the Taylor Dome site and Dye 3 which is not apparent in our data. It is also to mention that the relative range of variation in the ^{10}Be concentration record from the Dronning Maud Land ($\approx 0.7\text{–}1.6 \times 10^4$ atoms g^{-1}) is smaller than that shown by Steig *et al* (1996) for the Taylor Dome ($\approx 1\text{–}2.5 \times 10^4$ atoms g^{-1}) over the same time interval. Geographic and geomorphologic variability between the two sites may be the explanation for this difference. We also could not make direct comparison between our ^{10}Be flux and that of the Taylor Dome due to absence of such data from the latter site.

In Dye 3, Beer *et al* (1990), used statistically filtered ^{10}Be concentrations (atoms g^{-1}) instead of flux for the correlation with sunspot number and aa index. The plot of our ^{10}Be flux shows a surprisingly good match between our flux data and the Dye 3 (figure 7). Irrespective of minor seasonal shifts (≈ 0.5 year) between the data sets, a clear misfit occurs at the period 1978–1984. Instead of a reduced ^{10}Be concentration/flux during a high solar activity period, the Dye 3 data indicate enhancement in this period. This suggests that one or both (Dye 3 and Renland/Dronning Maud Land) the time scales have apparently captured a signal other than the solar modulation. The ^{10}Be flux should reflect more genuinely, than the ^{10}Be concentration, the solar modulation effect. But as discussed above, part of the variability may relate to the effects of the geomagnetic field intensity and climate. Another possibility is the erosion/redeposition of snow and, at depths below a few meters, even local snow melting may contribute to distortion of the primary signals. Distortion of the oxygen isotope data is apparent on both the Renland and DML records (figure 2a and b) and is expected to give rise to some errors (1–2 years) in the assignment of ages (Johnsen *et al* 1992). It is also expected that the relatively lower accumulation rates of the DML core may be more sensitive to local distortion (diffusion effect) of the annual layers which is also evident by the gradual decrease in the range of δ^{18}O seasonal variability (figure 2a). However, given the limited amount of data on ^{10}Be and still not well defined local effects of snow accumulation rates and ice dynamics (in Greenland and Antarctica), a perfect match between all the ^{10}Be profiles cannot be expected. Nevertheless, the data of this study suggest that the variation in ^{10}Be of the polar ice is mainly tied to solar modulation effects and offers an independent and important parameter in the correlation of short (annually and even less) and long (decades and centuries) variations in solar/climatic factors.

Acknowledgements

Financial support for this work was provided by the Swedish Natural Science Research Council (NFR), Knut and Alice Wallenberg Foundation and the Tandem Laboratory (AMS group). Data of Dye 3 were kindly provided by Dr. Jürg Beer. We thank Prof. D Lal for comments on this paper.

Appendix 1. ^{10}Be and accumulation rate data of the Renland and DML ice cores.

Year	Depth m	Acc. rate[a] ice/snow $cm\,y^{-1}$	Acc. rate w. eq. $cm\,y^{-1}$	^{10}Be atoms g^{-1}	Error atoms g^{-1}	^{10}Be flux atoms $cm^{-2}\,y^{-1}$	Error atoms $cm^{-2}\,y^{-1}$
Renland ice core							
1931	41.0	54.0	49.6	2.6e + 04	1776	1.28e + 06	88040
1932	40.5	54.0	49.6	2.1e + 04	1580	1.04e + 06	78343
1933	39.8	62.0	56.9	8.8e + 03	812	5.00e + 05	46243
1934	39.2	40.0	36.7	2.4e + 04	2848	8.82e + 05	1.05e + 05
1935	38.7	40.0	36.7	1.6e + 04	1368	5.80e + 05	50245
1936	38.3	31.0	28.5	8.9e + 03	1037	2.52e + 05	29512
1937	37.9	35.0	32.1	1.5e + 04	1659	4.66e + 05	53307
1938	37.5	61.0	56.0	1.5e + 04	1834	8.39e + 05	1.03e + 05
1939	36.8	60.0	55.1	9.1e + 03	1207	5.02e + 05	66494
1940	36.1	43.0	39.5	1.2e + 04	1153	4.69e + 05	45514
1941	35.6	63.0	57.8	7.0e + 03	1026	4.07e + 05	59338
1942	34.8	46.0	42.2	1.3e + 04	978	5.32e + 05	41317
1943	34.3	33.0	30.3	1.3e + 04	1338	3.84e + 05	40535
1944	33.9	62.0	56.9	1.1e + 04	1008	6.18e + 05	57379
1945	33.2	41.0	37.6	1.1e + 04	1139	4.28e + 05	42870
1946	32.7	53.0	48.7	1.1e + 04	1024	5.42e + 05	49836
1947	32.0	61.0	56.0	9.1e + 03	801	5.07e + 05	44887
1948	31.2	36.0	33.0	1.0e + 04	1279	3.41e + 05	42268
1949	30.8	44.0	40.4	3.8e + 03[b]	1540	1.54e + 05	62204
1950	30.2	40.0	36.7	1.4e + 04	1871	5.08e + 05	68703
1951	29.8	35.0	32.1	1.7e + 04	1446	5.47e + 05	46460
1952	29.3	51.0	46.8	1.3e + 04	1229	6.01e + 05	57548
1953	28.6	70.0	64.3	1.5e + 04	1407	9.46e + 05	90435
1954	27.7	46.0	42.2	8.0e + 03[b]	2827	3.39e + 05	1.20e + 05
1955	27.1	65.0	59.7	1.6e + 04	1697	9.60e + 05	1.01e + 05
1956	26.3	42.0	38.6	1.7e + 04	1781	6.47e + 05	68668
1957	25.8	75.0	68.9	2.0e + 04	1235	1.34e + 06	85011
1958	24.7	44.0	40.4	9.6e + 03[b]	2295	3.88e + 05	92682
1959	24.1	77.0	70.7	1.9e + 04	2760	1.31e + 06	1.95e + 05
1960	23.1	44.0	40.4	1.2e + 04	944	5.03e + 05	38141
1961	22.5	58.0	53.2	9.8e + 03	913	5.23e + 05	48619
1962	21.7	39.0	35.8	1.9e + 04	2054	6.93e + 05	73551
1963	21.1	50.0	45.9	1.8e + 04	1572	8.14e + 05	72177
1964	20.5	42.0	38.6	2.1e + 04	1795	7.99e + 05	69192
1965	19.9	42.0	38.6	2.0e + 04	1677	7.90e + 05	64654
1966	19.2	24.0	22.0	1.9e + 04	2067	4.08e + 05	45540
1967	18.9	41.0	37.6	2.0e + 04	2480	7.64e + 05	93335
1968	18.3	27.0	24.8	1.7e + 04	1786	4.28e + 05	44256
1969	17.9	51.0	46.8	1.1e + 04	624	5.00e + 05	29239
1970	17.1	44.0	40.4	1.0e + 04	1176	4.07e + 05	47501
1971	16.5	44.0	40.4	1.7e + 04	2095	7.07e + 05	84623
1972	15.9	79.0	72.5	9.5e + 03	860	6.86e + 05	62387
1973	14.6	33.0	30.3	1.8e + 04	1575	5.56e + 05	47727
1974	14.1	68.0	62.4	1.1e + 04	882	7.15e + 05	55033
1975	13.1	38.0	34.9	1.2e + 04	1089	4.12e + 05	37994
1976	12.5	67.0	61.5	1.1e + 04	1449	6.88e + 05	89151
1977	11.4	50.0	45.9	1.2e + 04	1702	5.71e + 05	78107
1978	10.6	50.0	45.9	6.9e + 03[b]	1235	3.15e + 05	56687
1979	9.85	43.0	39.5	1.1e + 04	1049	4.39e + 05	41413
1980	9.15	62.0	56.9	3.9e + 03	549	2.21e + 05	31230
1981	8.10	40.0	36.7	1.2e + 04	1038	4.57e + 05	38100
1982	7.40	56.0	51.4	8.0e + 03	926	4.10e + 05	47613
1983	6.40	43.0	39.5	1.5e + 04	1538	5.83e + 05	60693
1984	5.60	75.0	68.9	9.1e + 03[b]	1540	6.25e + 05	1.06e + 05
1985	4.15	45.0	41.3	1.4e + 04	1347	5.68e + 05	55657
1986	3.25	53.0	48.7	7.8e + 03[b]	1766	3.82e + 05	85946
1987	2.15	26.0	23.9	6.9e + 03[b]	1179	1.64e + 05	28140
Dronning Maud Land (DML) ice core[c]							
1932	30.4	29.0	22.0				
1933	30.1	30.0	23.0				

(*Continued*)

Appendix 1. (*Continued*)

Year	Depth m	Acc. rate[a] ice/snow cm y^{-1}	Acc. rate w. eq. cm y^{-1}	^{10}Be atoms g^{-1}	Error atoms g^{-1}	^{10}Be flux atoms cm^{-2} y^{-1}	Error atoms cm^{-2} y^{-1}
1934	29.8	40.0	31.0				
1935	29.4	56.0	43.0	1.5e + 04	1072	6.41e + 05	46096
1936	28.9	64.0	48.0				
1937	28.2	76.0	59.0	1.4e + 04	1648	8.50e + 05	97232
1938	27.5	99.0	79.0	8.1e + 03	410	6.38e + 05	32390
1939	26.5	79.0	58.0	1.3e + 04	597	7.66e + 05	34626
1940	25.7	71.0	53.0	1.2e + 04	412	6.52e + 05	21836
1941	25.0	47.0	35.0				
1942	24.5	24.0	18.0				
1943	24.2	33.0	24.0	2.9e + 04[b]	4320	6.89e + 05	1.04e + 05
1944	23.9	35.0	21.0				
1945	23.6	43.0	37.0				
1946	23.1	39.0	28.0				
1947	22.7	48.0	34.0				
1948	22.3	33.0	24.0	1.3e + 04	745	3.22e + 05	17880
1949	21.9	55.0	38.0	1.4e + 04	1006	5.31e + 05	38230
1950	21.4	42.0	25.0	2.2e + 04[b]	3498	5.56e + 05	87450
1951	21.0	90.0	58.0	1.3e + 04	605	7.56e + 05	35090
1952	20.1	102	73.0	1.4e + 04	849	9.99e + 05	62021
1953	19.0	46.0	31.0	1.3e + 04	928	4.15e + 05	28778
1954	18.6	35.0	24.0	1.5e + 04	1961	3.51e + 05	47061
1955	18.2	51.0	35.0	1.6e + 04	2160	5.56e + 05	75600
1956	17.7	53.0	36.0				
1957	17.2	31.0	21.0	8.4e + 03	1218	1.76e + 05	25578
1958	16.9	59.0	41.0	6.9e + 03	358	2.83e + 05	14700
1959	16.3	84.0	56.0	1.3e + 04	1682	7.42e + 05	94200
1960	15.4	39.0	26.0	1.2e + 04	982	3.05e + 05	25544
1961	15.1	44.0	28.0	7.9e + 03	647	2.20e + 05	18118
1962	14.6	36.0	20.0	9.1e + 03	846	1.82e + 05	16920
1963	14.2	50.0	29.0	1.3e + 04	805	3.86e + 05	23345
1964	13.7	35.0	23.0	1.3e + 04	1485	3.00e + 05	34154
1965	13.4	88.0	57.0	1.2e + 04	795	6.71e + 05	45318
1966	12.5	48.0	30.0	1.6e + 04	1265	4.90e + 05	37956
1967	12.0	42.0	26.0	1.2e + 04	869	3.02e + 05	22607
1968	11.6	74.0	47.0	1.5e + 04	1055	7.25e + 05	49585
1969	10.9	42.0	25.0	9.6e + 03	770	2.41e + 05	19252
1970	10.4	28.0	17.0	8.4e + 03	647	1.44e + 05	11001
1971	10.1	42.0	25.0	8.4e + 03	647	2.11e + 05	16179
1972	9.78	54.0	33.0	8.9e + 03	497	2.95e + 05	16424
1973	9.15	52.0	31.0	1.4e + 04	1769	4.42e + 05	54839
1974	8.68	34.0	20.0	1.4e + 04	1769	2.85e + 05	35380
1975	8.34	25.0	15.0	1.5e + 04	577	2.22e + 05	8655
1976	8.07	70.0	40.0	1.5e + 04	577	5.91e + 05	23081
1977	7.39	60.0	34.0	1.2e + 04	859	4.04e + 05	29229
1978	6.79	40.0	23.0	7.7e + 03	504	1.77e + 05	11592
1979	6.39	25.0	14.0	1.5e + 04	724	2.11e + 05	10149
1980	6.14	30.0	16.0	1.5e + 04	724	2.41e + 05	11599
1981	5.89	50.0	28.0	1.4e + 04	539	3.81e + 05	15098
1982	5.34	75.0	43.0	8.4e + 03	468	3.61e + 05	20161
1983	4.59	57.0	31.0	1.1e + 04	716	3.38e + 05	22196
1984	4.02	45.0	23.0	1.2e + 04	958	2.68e + 05	22036
1985	3.57	62.0	32.0	1.6e + 04	891	5.11e + 05	28537
1986	2.97	38.0	19.0	1.1e + 04	664	2.01e + 05	12616
1987	2.57	46.0	23.0	1.1e + 04	713	2.53e + 05	16399
1988	2.11	38.0	18.0	1.0e + 04	656	1.80e + 05	11813

[a] The accumulation rate is reported as ice for the Renland and as snow for the DML.
[b] A large error (> 15%) accompanies these samples, because of small amount of Be recovered. Thus they were excluded from the figures, except the start year (1987) for the Renland.
[c] Because of a small amount of sample, the years 1932–1934 were not analysed for ^{10}Be. Samples of the years 1941, 1942, 1944, 1945, 1946, 1947 were unluckily missed during preparation for the Be recovery.

References

Aldahan A and Possnert G 1993a Some analytical potential of the accelerator mass spectrometer at Uppsala University; 1st Internat. Symp. Applied Isotope Geochemistry, Geiranger, Norway (abstract)

Aldahan A and Possnert G 1993b ^{10}Be measurements with the Uppsala tandem accelerator and some geological applications; 1st Internat. Symp. Applied Isotope Geochemistry, Geiranger, Norway (abstract)

Aldahan A, Possnert G, Johnsen S J, Clausen H B, Isaksson E and Karlén W 1995 ^{10}Be and the 11-year solar cycle in ice records covering last 60 years; *Annales Geophysicae, supp.* **13** 422 (abstract)

Beer J, Blinov A, Bonani G, Finkel R C, Hofmann H J, Lehmann B, Oeschger H, Sigg A, Schwander J, Staffelbach T, Stauffer B, Suter M and Wölfli W 1990 Use of ^{10}Be in polar ice to trace the 11-years cycle of the solar activity; *Nature* **347** 164–166

Chambers J M 1993 *Graphical methods for data analysis*; (California; Wadsworth and Brooks)

Currie R 1987 Examples and implications of 18.6 – and 11-year terms in world weather records; In Climate: history, periodicity and predictability (eds) M R Rampino, W S Newman, J E Sanders and L K Konigsson (New York; Van Nostrand, Reinhold) pp. 379–403

Currie R 1994 Variance contribution to luni-solar and solar cycle signals in the St Lawrence and Nile river records; *Internat. J. Climatology* **14** 843–852

Isaksson E, Karlén W, Gundestrup N, Mayewski P, Whitlow S and Twickler M 1996 A century of accumulation and temperature change in Dronning Maud Land, Antarctica; *J. Geophys. Res.* **101** (D3) 7085–7094

Johnsen S J, Clausen H B, Dansgaard W, Gundestrup N S, Hansson M, Jonsson P, Steffensen J P and Sveinbjornsdottir E A 1992 A deep ice core from East Greenland; *Meddelelser om Gronland, Geosciences* **29** 1–22

Lal D and Peters B 1967 Cosmic ray produced radioactivity on the earth: In *Handbuch der physik 46* (Berlin; Springer-Verlag) pp. 551–612

Lal D 1987 ^{10}Be in polar ice: data reflect changes in cosmic ray flux or polar meteorology; *Geophys. Res. Lett.* **14** 785–788

Lal D 1992 Expected secular variation in the global terrestrial production rate of radiocarbon; In *The last deglaciation: absolute and Radiocarbon Chronologies.* (eds) E Bard and W S Broecker (Berlin; Springer-Verlag) pp. 113–125

Lal D and Jull A J T 1992 Cosmogenic nuclides in ice sheets; *Radiocarbon* **34** 227–233

Monaghan M, Krishnaswami S and Turkian K K 1986 The global-average production rate of ^{10}Be; *Earth Planet. Sci. Lett.* **76** 279–287

Royer T C 1993 High latitude oceanic variability associated with the 18.6-year luni-solar tide; *J. Geophys. Res.* **98** 4639–4644

Seleshi Y, Demaree G R and Delleur J W 1994 Sunspot numbers as a possible indicator of annual rainfall at Addis Ababa, Ethiopia; *Internat. J. Climatology* **14** 911–923

Solar-geophysical data reports 1994 Editor (Coffey E H) National Oceanic and Atmospheric Administration, Boulder, Colorado

Steig E J, Polissar P J, Stuiver M, Groots P M and Finkel R C 1996 Large amplitude solar modulation cycles of ^{10}Be in Antarctica: implication for atmospheric mixing processes and interpretation of the ice core record; *Geophys. Res. Lett.* **23** 523–5266

Stuiver M and Braziunas T F 1993 Sun, ocean, climate and atmosphere $^{14}CO_2$: an evaluation of causal and spectral relationship; *The Holocene* **3,4** 289–305

Stuiver M, Grootes P M and Braziunas T F 1995 The GISP2 $\delta^{18}O$ climate record of the past 16,500 years and the role of the sun, ocean, and volcanoes; *Quat. Res.* **44** 341–354

MS received 6 October 1997; revised 21 February 1998